

Biophysical Journal, Volume 123

Supplemental information

Dark nanodiscs for evaluating membrane protein thermostability by differential scanning fluorimetry

Jazlyn A. Selvasingh, Eli F. McDonald, Preston D. Neuffer, Jacob R. McKinney, Jens Meiler, and Kaitlyn V. Ledwitch

1 **Supplemental Materials for Dark nanodiscs for evaluating membrane protein thermostability**
2 **by differential scanning fluorimetry**
3

4 Jazlyn A. Selvasingh^{1,2}, Eli F. McDonald^{1,2}, Preston D. Neuffer^{1,2}, Jacob R. McKinney^{1,2}, Jens Meiler^{1,2,3*}, Kaitlyn
5 V. Ledwitch^{1,2,4*}

6 ¹Center for Structural Biology, Vanderbilt University, Nashville, TN 37240, USA

7 ²Department of Chemistry, Vanderbilt University, Nashville, TN 37235, USA

8 ³Institute of Drug Discovery, Faculty of Medicine, University of Leipzig, 04103 Leipzig, Germany

9 ⁴Lead contact, k.ledwitch@vanderbilt.edu

10

11

12 Table of Contents

13

14 Supplemental Table(s)

2

15

16 Supplemental Figures

3-7

17 **Table S1**

Sample	[free thiol]	free thiol (%)
DsbB – DPC micelle	2.15 +/- 0.29 μ M	2.25 %
DsbB – dark nanodisc	1.52 +/- 0.19 μ M	1.59 %

18

19 **Table S1. Quantification of free thiol content for DsbB in DPC micelles compared to dark nanodiscs.** The
20 Measure-IT™ Thiol Assay Kit was utilized to quantify the free thiol content of DsbB in micelles versus DsbB
21 reconstituted in dark nanodiscs. Each sample was run in triplicate (n=3) at a DsbB protein concentration of 1
22 mg/mL. The dark membrane scaffold protein does not contribute to the thiol measurement because there is no
23 cysteine content in the dark nanodisc construct.

24

25

26

27

28

29

30

31

32

33

34

35

36

37

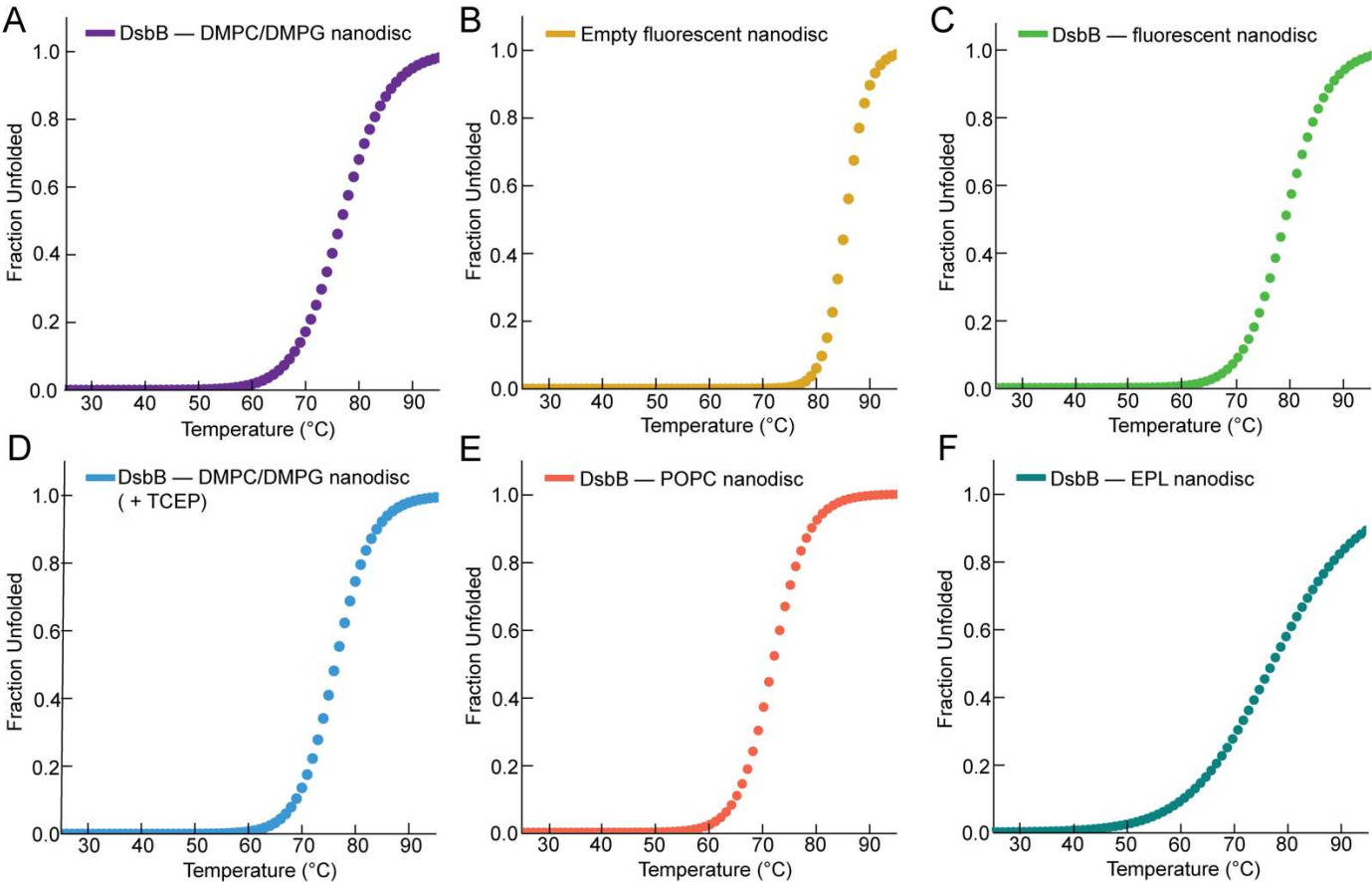
38

39

40

41

42



44

45 **Figure S1. Fraction unfolded plotted as a function of temperature for the nanodisc samples evaluated in**
 46 **this study.** For visualization, baseline-corrected experimental curves were calculated from the rate constant of
 47 the unfolding transition, the rate constant of the baseline transition, baseline noise, and baseline offset. Fraction
 48 unfolded plots are shown for (A) DsbB in a dark nanodisc (DMPC/DMPG), (B) empty fluorescent nanodisc
 49 (DMPC/DMPG), (C) DsbB in an MSP1D1 fluorescent nanodisc (DMPC/DMPG), (D), DsbB in a dark nanodisc
 50 (DMPC/DMPG) under reducing conditions. (E) DsbB in a dark nanodisc (POPC), (F) DsbB in a dark nanodisc
 51 (*E. coli* Polar Lipid Extract).

52

53

54

55

56

57

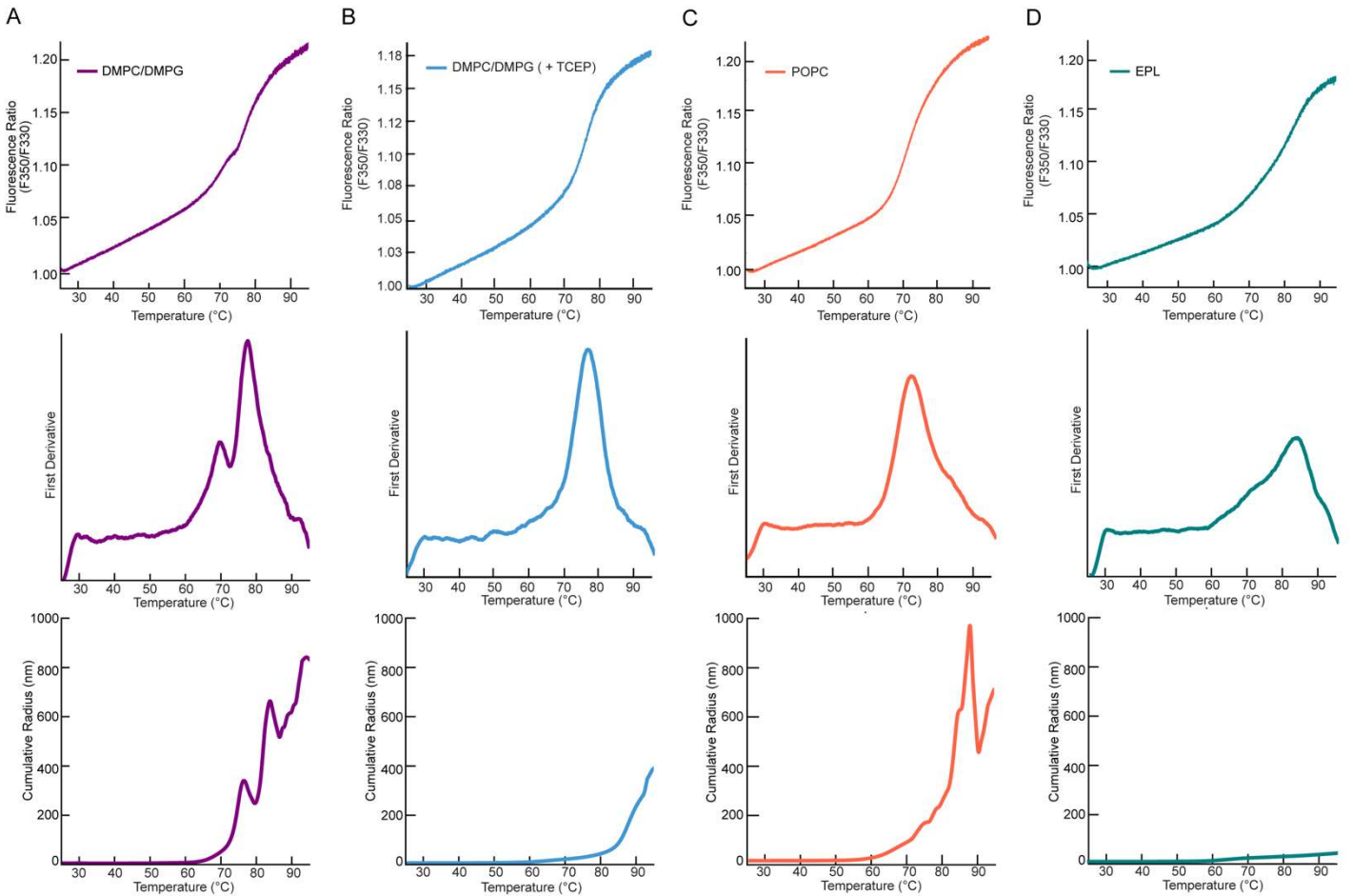
58

59

60

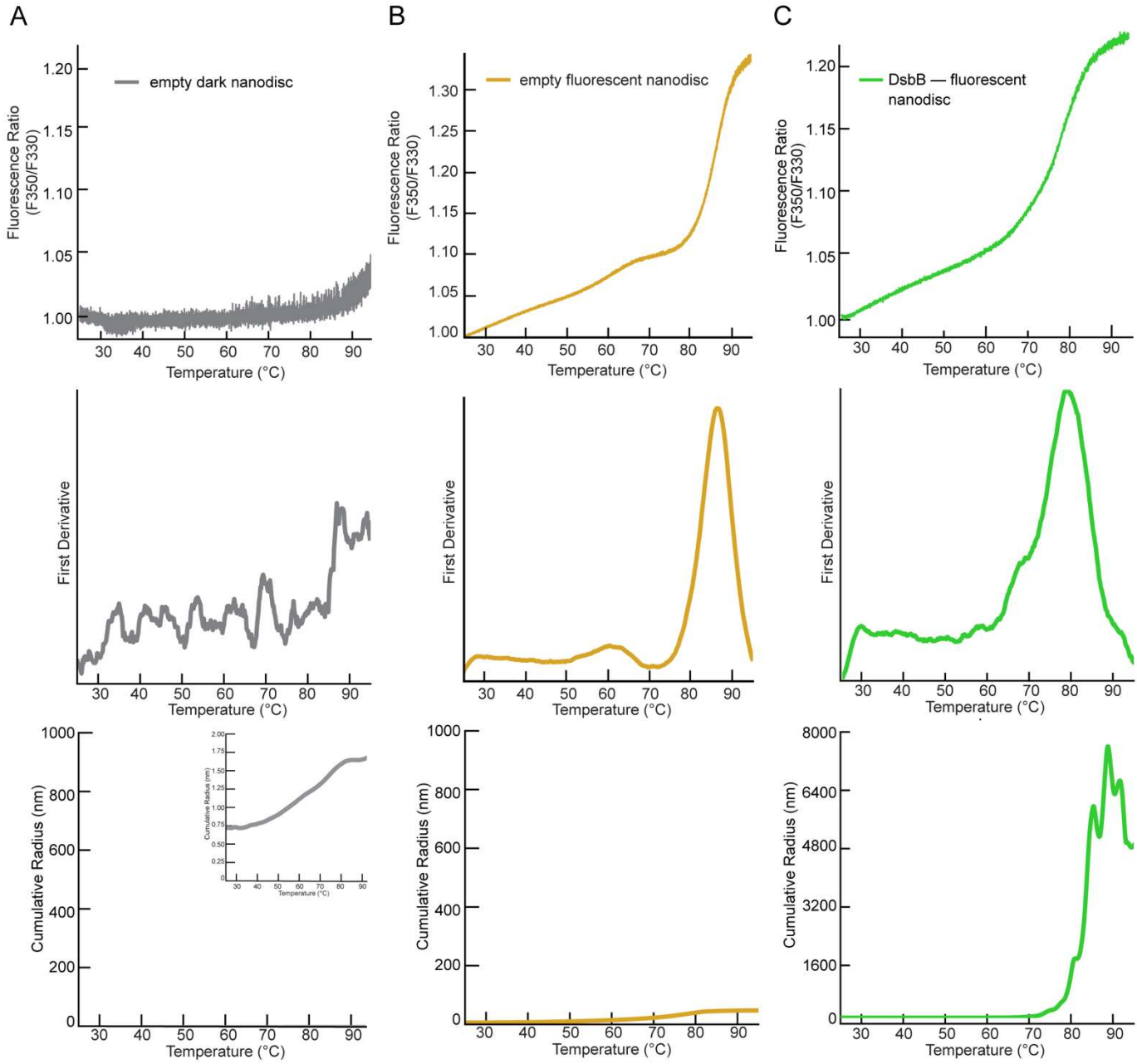
61

62 **Figure S2**



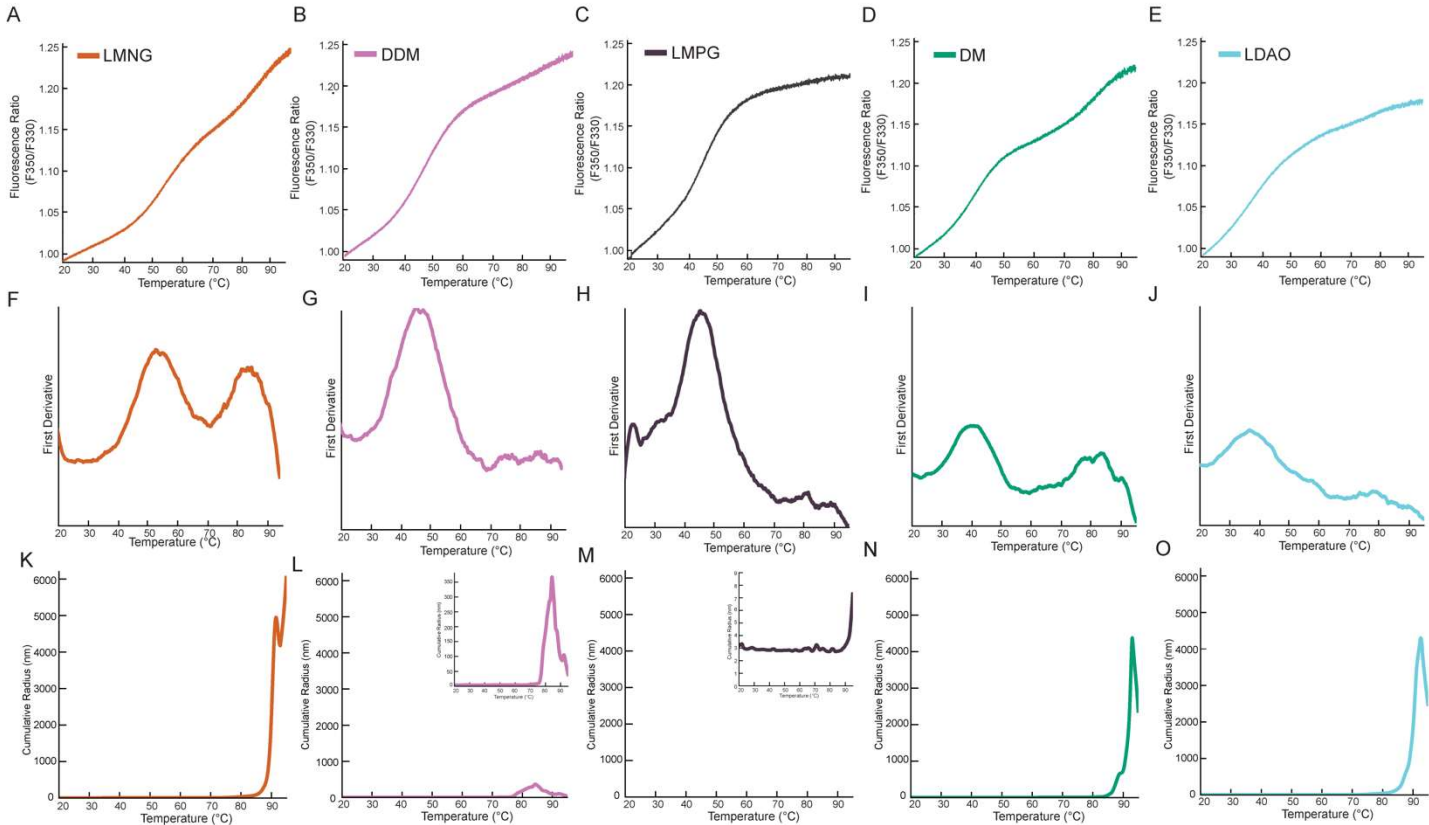
63
64 **Figure S2. NanoDSF unfolding curves, first derivative, and cumulative radius plots for each dark**
65 **nanodisc condition. (A)** DsbB in a dark nanodisc (DMPC/DMPG), **(B)** DsbB in a dark nanodisc (DMPC/DMPG)
66 under reducing conditions. **(C)** DsbB in a dark nanodisc (POPC), and **(D)** DsbB in a dark nanodisc (*E. coli* Polar
67 Lipid Extract). **Top row:** The F350/F330 thermal unfolding curves for each of the nanodisc samples. **Second**
68 **row:** The first derivative plots for each nanodisc sample. **Third row:** The cumulative radius plots from dynamic
69 light scattering measurements collected in tandem with the fluorescence measurements. All samples were run
70 in triplicate (n=3) and the average is plotted.

71
72
73
74
75
76
77
78
79
80

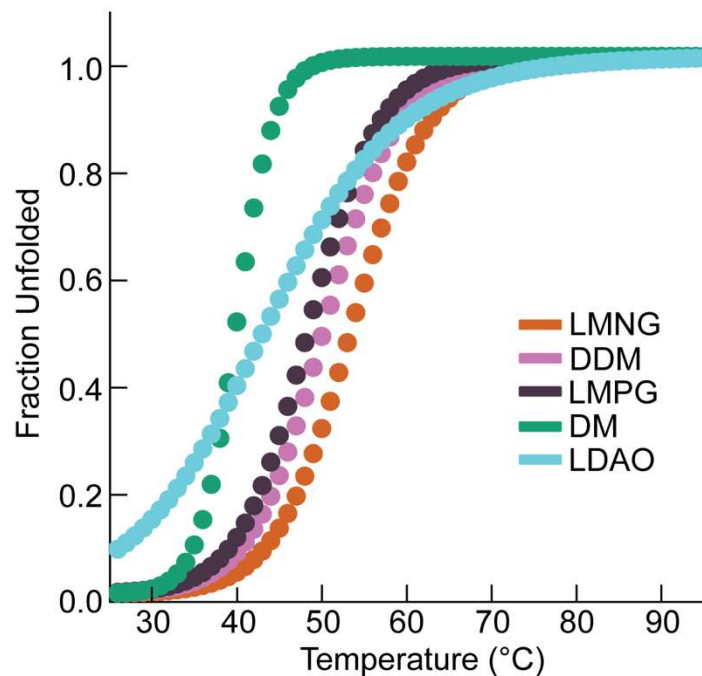


82
83 **Figure S3. NanoDSF unfolding curves, first derivative, and cumulative radius plots for all nanodisc**
84 **control samples. (A)** empty dark nanodisc, **(B)** empty fluorescent MSP1D1 nanodisc, and **(C)** DsbB in a
85 fluorescent MSP1D1 nanodisc. All control nanodisc samples were loaded with DMPC/DMPG lipids. **Top row:**
86 The F350/F330 thermal unfolding curves for each of the nanodisc samples. **Second row:** The first derivative
87 plots for each nanodisc sample. **Third row:** The cumulative radius plots from dynamic light scattering
88 measurements collected in tandem with the fluorescence measurements. All samples were run in triplicate (n=3)
89 and the average is plotted.

90
91
92



94
95 **Figure S4. NanoDSF unfolding curves, first derivative, and cumulative radius plots for detergent-**
96 **solubilized DsbB under a panel of micelle conditions. (A) LMNG, (B) DDM, (C) LMPG, (D) DM, and (E)**
97 **LDAO. A-E:** The F350/F330 thermal unfolding curves for detergent-solubilized DsbB under a panel of different
98 micelle conditions. **F-J:** The first derivative plots for detergent-solubilized DsbB. The inflection points correspond
99 to T_m values of 56.4 ± 0.9 °C (LMNG, orange), 49.5 ± 1.0 °C (DDM, pink), 45.4 ± 0.1 °C (LMPG, dark purple),
100 40.1 ± 0.9 °C (DM, green), and 36.7 ± 0.2 °C (LDAO, cyan). **K-O:** The cumulative radius plots from dynamic light
101 scattering measurements collected in tandem with fluorescence measurements. All samples were run in triplicate
102 ($n=3$) and the average is plotted.



113

114

115

116

117

118

Figure S5. Fraction unfolded plotted as a function of temperature for detergent-solubilized DsbB under a panel of different detergent micelle conditions. The fraction unfolded is plotted for DsbB under a panel of different detergent micelle conditions including LMNG, DDM, LMPG, DM, and LDAO. For visualization, baseline-corrected experimental curves were calculated from parameters derived after fitting the data to an equilibrium two-state unfolding model in MoltenProt.